The Journal of Immunology

A Critical Role for $P2X_7$ Receptor–Induced VCAM-1 Shedding and Neutrophil Infiltration during Acute Lung Injury

Amarjit Mishra, Yujie Guo, Li Zhang, Sunil More, Tingting Weng, Narendranath Reddy Chintagari, Chaoqun Huang, Yurong Liang, Samuel Pushparaj, Deming Gou, Melanie Breshears and Lin Liu

J Immunol 2016; 197:2828-2837; Prepublished online 24 August 2016;
doi: 10.4049/jimmunol.1501041
http://www.jimmunol.org/content/197/7/2828

The Journal of Immunology is published twice each month by
The American Association of Immunologists, Inc.,
1451 Rockville Pike, Suite 650, Rockville, MD 20852

Print ISSN: 0022-1767 Online ISSN: 1550-6606.

A Critical Role for $P2X_7$ Receptor–Induced VCAM-1 Shedding and Neutrophil Infiltration during Acute Lung Injury

Amarjit Mishra,* Yujie Guo,*,† Li Zhang,* Sunil More,*,† Tingting Weng,* Narendranath Reddy Chintagari,* Chaoqun Huang,*,† Yurong Liang,*,† Samuel Pushparaj,*,† Deming Gou,‡ Melanie Breshears,†,§ and Lin Liu*,†

Pulmonary neutrophils are the initial inflammatory cells that are recruited during lung injury and are crucial for innate immunity. However, pathological recruitment of neutrophils results in lung injury. The objective of this study is to determine whether the novel neutrophil chemoattractant, soluble VCAM-1 (sVCAM-1), recruits pathological levels of neutrophils to injury sites and amplifies lung inflammation during acute lung injury. The mice with $P2X_7$ receptor deficiency, or treated with a $P2X_7$ receptor inhibitor or anti–VCAM-1 Abs, were subjected to a clinically relevant two-hit LPS and mechanical ventilation–induced acute lung injury. Neutrophil infiltration and lung inflammation were measured. Neutrophil chemotactic activities were determined by a chemotaxis assay. VCAM-1 shedding and signaling pathways were assessed in isolated lung epithelial cells. Ab neutralization of sVCAM-1 or deficiency or antagonism of $P2X_7R$ reduced neutrophil infiltration and proinflammatory cytokine levels. The ligands for sVCAM-1 were increased during acute lung injury. sVCAM-1 had neutrophil chemotactic activities and activated alveolar macrophages. VCAM-1 is released into the alveolar airspace from alveolar epithelial type I cells through $P2X_7$ receptor–mediated activation of the metalloproteinase ADAM-17. In conclusion, sVCAM-1 is a novel chemoattractant for neutrophils and an activator for alveolar macrophages. Targeting sVCAM-1 provides a therapeutic intervention that could block pathological neutrophil recruitment, without interfering with the physiological recruitment of neutrophils, thus avoiding the impairment of host defenses. ***The Journal of Immunology*****, 2016, 197: 2828–2837.**

Acute lung injury (ALI), the severe form of which is referred to as acute respiratory distress syndrome (ARDS), is a progressive syndrome that develops directly from pneumonia, gastric acid aspiration, or inhalation of toxic gases, or indirectly from extrapulmonary sepsis or trauma. ALI/ARDS is characterized by acute inflammation with neutrophil infiltration, alveolar-capillary barrier damage, pulmonary edema, and arterial hypoxemia (1).

Migration of neutrophils into the lungs is central to the pathogenesis of ALI/ARDS. Neutrophils play an important role in innate immunity by phagocytizing microbes. However, excessive recruitment and prolonged activation of neutrophils often lead to lung injury, including endothelial and epithelial cell damage through the extracellular release of antimicrobial agents such as reactive oxygen species, proteases, and cationic peptides (2). As such, neutrophils represent a double-edged sword. In some cases, neutrophils can be recruited to the lungs without damaging the lung tissue (3, 4), whereas in some, but not all animal models, depletion of neutrophils reduces lung injury and bacterial clearance (5–7). These findings give rise to the question of whether there are both good, or physiological, neutrophils and bad, or pathological, neutrophils.

IL-8 in humans and keratinocyte-derived chemokine and MIP-2 in mice are the major chemokines for neutrophils in the lung (2). Two additional chemokines, LIX and lungkine, also play important roles in neutrophil recruitment in lung infections (8, 9). Furthermore, proline-glycine-proline has recently been identified as a neutrophil chemoattractant involved in chronic neutrophilic inflammation (10). However, it is unclear whether these chemokines/chemoattractants are responsible for the recruitment of physiological or pathological neutrophils.

The migration of neutrophils across the endothelium is mediated by the firm adhesion of neutrophils to the endothelial cells through the interaction of β_2 integrins on circulating neutrophils and ICAM-1 on activated endothelial cells. However, β_2 integrin–independent pathways have also been observed (11–13). The extent to which a certain pathway is used depends on the stimulus. The $\alpha_4\beta_1$ integrins, which are the ligands for VCAM-1, are highly expressed in mononuclear leukocytes, but are induced on neu-

*Lundberg-Kienlen Lung Biology and Toxicology Laboratory, Department of Physiological Sciences, Oklahoma State University, Stillwater, OK 74078; †Oklahoma Center for Respiratory and Infectious Diseases, Oklahoma State University, Stillwater, OK 74078; ‡Shenzhen Key Laboratory of Microbial Genetic Engineering, College of Life Sciences, Shenzhen University, Shenzhen, Guangdong 518060, China; and §Department of Pathobiology, Oklahoma State University, Stillwater, OK 74078

ORCIDs: 0000-0002-3777-0338 (A.M.); 0000-0001-5007-8795 (S.M.); 0000-0002-5746-280X (S.P.); 0000-0002-3312-841X (D.G.); 0000-0002-4811-4897 (L.L.).

Received for publication May 20, 2015. Accepted for publication July 25, 2016.

This work was supported by National Heart, Lung, and Blood Institute Awards R01HL071628 and R01HL116876 and by the Oklahoma Center for the Advancement of Science and Technology (to L.L.), and the Core facilities used were supported by National Institute of General Medical Sciences Award P20GM103648.

The content is solely the responsibility of the authors and does not necessarily represent the official views of the National Institutes of Health.

Address correspondence and reprint requests to Dr. Lin Liu, 264 McElroy Hall, Department of Physiological Sciences, Oklahoma State University, Stillwater, OK 74078. E-mail address: lin.liu@okstate.edu

The online version of this article contains supplemental material.

Abbreviations used in this article: AEC I, alveolar epithelial type I cell; AEC II, alveolar epithelial type II cell; ALI, acute lung injury; ARDS, acute respiratory distress syndrome; BAL, bronchoalveolar lavage; EB, Evans blue; MMP, matrix metalloproteinase; MV, mechanical ventilation; $P2X_7R$, purinergic $P2X_7$ receptor; sVCAM-1, soluble VCAM-1.

trophils under certain pathological conditions (14, 15). However, the functional roles of this induction are still unclear.

The purinergic $P2X_7$ receptor ($P2X_7R$) is an ATP-gated cation channel. Several studies have observed the involvement of $P2X_7R$ in lung inflammation due to its role in processing IL-1β in macrophages (16–19). We have previously shown that $P2X_7R$ is specifically expressed in alveolar epithelial type I cells (AEC I), but not in alveolar epithelial type II cells (AEC II) of the lung parenchyme (20). We have also reported that $P2X_7R$ expressed in AEC I regulates lung surfactant secretion in AEC II (21).

In this study, we found that $P2X_7R^{-/-}$ mice exhibit reduced IL-1β expression levels and neutrophil infiltration in bronchoalveolar lavage (BAL) fluid from an ALI model. However, we did not observe any changes in the levels of known neutrophil chemokines. Further investigation led to the discovery that alveolar soluble VCAM-1 (sVCAM-1) shed from AEC I functions as a novel neutrophil chemoattractant during ALI. As the $\alpha_4\beta_1$ integrins responsible for the binding of VCAM-1 are induced during ALI, targeting alveolar sVCAM-1 is expected to provide a differential therapeutic intervention for ALI/ARDS by inhibiting $\alpha_4\beta_1$ integrin–mediated pathological neutrophil recruitment, without interfering with the normal β_2 integrin–mediated host defense system.

Materials and Methods

Mice

All animal procedures were approved by the Institutional Animal Care Committee of Oklahoma State University. Wild-type C57BL/6 and $P2X_7R^{-/-}$ (B6.129P2-P2rx7^{tm1}Gab/J) breeder mice were obtained from The Jackson Laboratory (Bar Harbor, ME) and bred in the Laboratory Animal Resource Unit of Oklahoma State University. Animals between 6 and 10 wk old were used for the experiments.

Murine model of acute lung injury

We employed a modified murine two-hit lung injury model involving a low dose of LPS pretreatment, followed by mechanical ventilation (MV) (22). Mice were randomly assigned to one of two groups: 1) the spontaneous breathing nonventilated control or 2) the LPS with MV (LPS plus MV) group. The mice were anesthetized with ketamine (80 mg/kg) and xylazine (10 mg/kg) i.p. A tracheotomy was performed through the soft tissue of the anterior neck to expose the trachea, and a 22-gauge needle was inserted into the trachea. The mice were placed in a supine position on a warming device with a heating lamp to maintain their body temperature at 37°C throughout the experiment. The mice were injected with pyrogen-free saline (1.5 μl/g) or LPS (*Escherichia coli* serotype 0111:B4, 0.5 μg/g bodyweight, 1.5 μl/g; Sigma-Aldrich) through the inserted needle. Sixty minutes after injection, the mice were ventilated for 150 min on a small animal ventilator (SAR-830/AP; CWE) with the following settings: respiratory rate = 125 breaths per minute; inspiratory and expiratory ratio = 1:2; tidal volume = 12 ml/kg bodyweight; positive end-expiratory pressure = 3 cm H_2O; and inspired oxygen fraction of 0.21. The mice were given xylazine and ketamine at half of the initial dose i.p. at 1-h intervals throughout the experiment to maintain adequate sedation.

In separate experiments, LPS was coadministered in the lungs (at a final volume of 1.5 μl/g bodyweight) with AZ10606120-dihydrochloride (a $P2X_7R$ antagonist, 100 μM; Tocris Biosci, Ellisville, MO), a functional blocking mAb against VCAM-1 (88 μg/mouse, purified rat anti-mouse CD-106; BD Pharmingen, San Diego, CA), and an isotype-matched control Ab (purified rat IgG2a κ isotype control; BD Pharmingen) in wild-type mice or a recombinant mouse VCAM-1 Ab (5 μg/mouse; R&D Systems, Minneapolis, MN) in $P2X_7R^{-/-}$ mice. After 60 min, the mice were ventilated for 150 min, as described above.

Bronchoalveolar lavage

BAL was performed three times using 1 ml 0.9% sterile saline. The recovered BAL fluids were pooled and centrifuged at 250 × *g* for 10 min. The BAL fluid was then subjected to analyses of total protein and cytokine contents. Cell pellets were cytospun at 600 × *g* for 10 min. The total cell number was counted with a standard hemocytometer. Differential cell counting was performed using a modified Wright Giemsa stain. A total of 500 cells was counted from randomly chosen fields in each sample. The total protein concentration in the BAL fluid was determined via the bicinchoninic acid method (BCA protein assay kit; Pierce, Rockford, IL) with BSA as the standard. The lung tissue was harvested, snap frozen in liquid nitrogen, and stored in aliquots at −80°C for biochemical and gene expression analyses.

Cytokine Ab array

BAL fluids from wild-type and $P2X_7R^{-/-}$ mice were assayed to determine their cytokine content using the RayBio Mouse Cytokine Ab Array (C-series 2000; RayBiotech, Norcross, GA), according to the manufacturer's instructions. Briefly, BAL fluids pooled from three mice in each group were added to preblocked protein array membranes, followed by overnight incubation at 4°C. The array membranes were then washed three times with wash buffer and incubated with biotin-conjugated anti-cytokine Abs for 2 h at room temperature. After washing, streptavidin-HRP was added, and the membranes were incubated for 2 h. The protein array membranes were subsequently incubated with detection buffer for 1 min and exposed to x-ray film. The resulting membrane films were quantified using the Quantity One software tool (Bio-Rad, Hercules, CA). To eliminate any loading differences, the average ODs of each cytokine were normalized to the average ODs of the biotin-conjugated positive control samples (upper left and lower right of each membrane).

ELISA

sVCAM-1, IL-1β, IL-6, MCP-1, and IgM concentrations in BAL and/or sera were determined via ELISA, according to the manufacturers' recommendations (mouse IgM ELISA kit, Bethyl Labs; Quantikine mouse IL-1β and sVCAM-1 immunoassay, R&D Systems; and mouse IL-6, TNF-α, and MCP-1 ELISA Ready-SET-Go, eBiosciences, San Diego, CA). Undiluted samples were used to maximize the detection level. The sensitivities were 1.37 ng/ml for IgM, 0.3 ng/ml for sVCAM-1, 4 pg/ml for IL-6, and 8 pg/ml for IL-1β and MCP-1.

Cell-based ELISA

A cell-based ELISA was used to determine the binding of sVCAM-1 to isolated rat alveolar macrophages. Alveolar macrophages (0.2×10^6/well) were plated in 96-well microtiter plates (Costar, Cambridge, MA) for 1 h and incubated with different concentrations of sVCAM-1 (0, 100, 1,000, and 10,000 ng/ml) for 45 min at 37°C. After being carefully washed with phosphate buffer solution, the cells were incubated for 1 h with a rabbit anti-rat VCAM-1 Ab (Abcam, Cambridge, MA) or a preimmune IgG fraction at a concentration of 50 μg/ml. Next, the cells were incubated with an anti-rabbit HRP-conjugated Ab (1:5,000 dilution; Amersham, Arlington Heights, IL) for 45 min. Color development was achieved via the addition of the *o*-phenylenediamine dihydrochloride substrate, and the reaction was stopped with 50 μl 3 M H_2SO_4. Finally, the absorbance at 490 nm was measured.

Nitrite and nitrate production

Rat alveolar macrophages were seeded at a density of 1×10^6/ml in 12-well culture plates in DMEM supplemented with 10% FBS, penicillin, and streptomycin. After 1 h of incubation, unattached cells were removed. The attached macrophages were then incubated with LPS (1 μg/ml) or VCAM-1 (10 μg/ml) for 4 h. The nitrite and nitrate concentrations in cell-free culture supernatants were determined via the Griess reaction after nitrate was converted to nitrite by NADPH-dependent nitrate reductase (23).

Lung tissue myeloperoxidase

Whole-lung tissue was homogenized in 1 ml 50 mM potassium phosphate (pH 6), followed by centrifugation at 14,000 × *g* for 15 min at 4°C. The pellet was then resuspended in phosphate buffer containing 50 mM hexadecyltrimethylammonium bromide. The samples were sonicated on ice for 20 s, freeze thawed twice, and centrifuged at 14,000 × *g* for 10 min at 4°C, and 100 μl undiluted sample was immediately added to 2.9 ml phosphate buffer containing 0.167 mg/ml *O*-danisidine dihydrochloride and 0.0005% hydrogen peroxide in cuvettes. Finally, the absorbance at 460 nm was measured for 5 min, and myeloperoxidase activity was expressed as the absorbance per minute per milligram of total protein.

Lung microvascular permeability

Lung microvascular permeability in wild-type and $P2X_7R^{-/-}$ mice was assessed using a modified Evans blue (EB) dye extravasation method, as previously described (24). EB dye (20 mg/kg body weight) was injected into the jugular vein of the animals after LPS injection, followed by

ventilation for 150 min, and the lungs were perfused with 1 ml 0.9% sterile saline via the right ventricle to remove the remaining blood from the pulmonary circulation. The lungs were then harvested and weighed, and the EB dye was extracted from lung homogenates after incubation with formamide (8 ml/g wet tissue) for 48 h at room temperature, followed by centrifugation at 2000 × *g* for 30 min. The concentration of EB dye in the lung tissue was quantified by measuring the absorbance at 620 nm based on a standard curve. The total amount of EB dye present in the pulmonary tissue was quantified and normalized to the tissue weight.

Histopathology

The lungs of wild-type and $P2X_7R^{-/-}$ mice were injected with 4% paraformaldehyde in PBS at 20 cm H_2O pressure, and then fixed for 48 h, embedded in paraffin, and sectioned into 4-μm–thick sections. The sections were stained with H&E and examined under a light microscope.

Isolation and culture of mouse AEC II

Mouse alveolar AEC II were isolated from wild-type and $P2X_7R^{-/-}$ mice, as described previously (25). The lungs were perfused free of blood with a solution containing 0.9% NaCl, 0.1% glucose, 10 mM HEPES (pH 7.4), 5 mM KCl, 1.3 mM $MgSO_4$, 1.7 mM $CaCl_2$, 0.1 mg/ml streptomycin sulfate, 0.06 mg/ml penicillin G, 3 mM Na_2HPO_4, and 3 mM NaH_2PO_4. AEC II were released from the lung via enzymatic digestion with 0.5 ml dispase (20 caseinolytic U/ml; BD Biosciences, Franklin Lakes, NJ) injected via the trachea for 15 min. Three individual lungs were isolated, minced, and pooled in a beaker. The lung slices were further digested with DNase I (100 μg/ml) for 45 min at 37˚C in a 50-ml beaker (~17 ml digestion mixture containing dispase and DNase I) with intermittent shaking. Next, the digested lungs were sequentially filtered through 160-, 37-, and 15-μm nylon meshes, and the filtrate was centrifuged at 250 × *g* for 10 min. The cell pellet was resuspended in DMEM and incubated in a 100-mm petri dish coated with mouse IgG (75 μg/dish) for 1 h. The cells were subsequently spun down at 250 × *g* for 10 min and resuspended in DMEM containing 10% FBS. The cell yield was ~10×10^6 per isolation (three mice), and the cell viability was >97%, as demonstrated via trypan blue exclusion. AEC II were then cultured in fibronectin-coated 12-well tissue culture plates at a concentration of 1×10^6 cells/well in DMEM supplemented with 10% FBS, penicillin, and streptomycin. AEC II were cultured for 3 d to allow them to *trans*-differentiate into AEC I. For dose–response experiments, cells cultured for 3 d were stimulated with IL-1β (0, 0.1, 1, 10, and 100 ng/ml; R&D Systems) for 24 or 48 h. In separate experiments, AEC cultured for 3 d were stimulated with IL-1β (10 ng/ml) in the presence or absence of the matrix metalloproteinase (MMP) inhibitor GM-60001 (50 μM; EMD Millipore, Billerica, MA) for 48 h, and the media were collected for the determination of sVCAM-1 levels via ELISA.

Isolation of mouse AEC I and AEC II

Mouse AEC I and AEC II were freshly isolated from C57BL/6 mice, according to our previously published protocol (21). Briefly, the lungs were perfused with a solution containing 0.9% NaCl, 0.1% glucose, 10 mM HEPES (pH 7.4), 5 mM KCl, 1.3 mM $MgSO_4$, 1.7 mM $CaCl_2$, 0.1 mg/ml streptomycin sulfate, 0.06 mg/ml penicillin G, 3 mM Na_2HPO_4, and 3 mM NaH_2PO_4, after which the lungs were isolated and injected with 1 ml digestion mixture (dispase, 20 caseinolytic U/ml, and elastase, 4 U/ml in solution) directly through the trachea. Three individual lungs were isolated and pooled in a beaker containing ~17 ml digestion mixture, followed by incubation at 37˚C for 15 min. After incubation, the lungs were minced, and the lung tissue was further digested with DNase I (100 μg/ml) for 45 min at 37˚C with intermittent shaking. The lung samples were then sequentially filtered through 160-, 37-, and 15-μm nylon meshes, and the filtrate was centrifuged at 250 × *g* for 10 min. The cell pellet was resuspended in DMEM and incubated for 1 h in a 100-mm petri dish coated with mouse IgG (75 μg/dish). The cells were subsequently centrifuged at 250 × *g* for 10 min and resuspended in DMEM containing 10% FBS. The cell yield was ~8×10^6 per mouse, and the cell viability was >95%. Freshly isolated cells contained ~31% AEC I and ~64% AEC II, similar to the percentages of AEC I and AEC II observed in vivo.

Flow cytometry

The surface expression of integrins on neutrophils was determined using a FITC-conjugated integrin α_4 Ab (catalogue 553156), an α_M Ab (catalogue 557396), an integrin β_7 Ab (catalogue 557494), and an isotype control Ab (rat IgG2b, κ, catalogue 553988; BD Pharmingen), as well as a PE-conjugated mAb against the murine granulocyte marker Gr-1 (RB6-8C5; BD Pharmingen) through FACS analysis. Blood neutrophils (1×10^6 cells in 100 μl staining buffer [PBS containing 1% BSA and 0.1% sodium azide]) or BAL cells (1×10^5 cells in 100 μl staining buffer) were incubated for 45 min at 4˚C with FITC- and PE-conjugated Abs. The cells were also labeled with isotype control rat anti-mouse IgG Abs. The cells were then washed twice with the staining buffer.

Freshly isolated AEC I and AEC II were stained with PE-conjugated podoplanin (an AEC I cell marker; BioLegend, San Diego, CA) and FITC-conjugated monoclonal VCAM-1 (Abcam). Fluorescence was determined on a single argon laser cytofluorometer FACSCalibur (BD Biosciences) and analyzed using CellQuest software. The granulocyte, lymphocyte, and monocyte (or macrophage) populations were discriminated based on the forward- and side-scattering properties of the three cell populations. Mean fluorescence intensity values were determined based on the histograms of the gated populations. The mean fluorescence was obtained by subtracting the measured control IgG fluorescence from the mean fluorescence for the population.

Chemotaxis assay

Peripheral rat blood neutrophils were isolated from EDTA anticoagulated whole blood collected via abdominal aortic puncture. Bone marrows were collected from the femur and tibia of C57BL/6 mice. RBCs were removed through hypotonic lysis. Neutrophils were purified via centrifugation using an OptiPrep density gradient (Sigma-Aldrich, St. Louis, MO) and resuspended in HBSS (2×10^7/ml).

Neutrophil chemotaxis assays were performed in duplicate using 3-μm membrane Transwell. Mouse recombinant VCAM-1 (R&D Systems) was diluted in HBSS and added to the lower wells (200 μl, 10 μg/ml) of the Transwell inserts. In some experiments, BAL fluid or 50% conditioned medium from cultured AEC II obtained from wild-type and $P2X_7^{-/-}$ mice was added to the lower chambers. Neutrophils were preactivated with 2.5 μM dihydrochalasin B (a known inducer of surface integrin expression) for 10 min. Next, 100 μl neutrophil solution (1×10^6 cells/ml) was added to the upper chambers. The loaded chambers were incubated at 37˚C in humidified air containing 5% CO_2 for 1 h. The membrane was then removed, fixed, and stained with a Wright Giemsa stain. The cells that migrated and adhered to the lower surface of the membrane were counted from 10 fields under the ×10 objective of the microscope (Olympus). The data were expressed as the number of neutrophils per field.

Western blotting

Lung homogenates and cell lysates were separated in a 10% SDS-polyacrylamide gel and transferred to a nitrocellulose membrane. The membrane was then stained with Ponceau S to ensure proper transfer and blocked overnight with 5% dry skim milk in 100 mM TBST. The membranes were incubated with anti-pERK1/2 and anti-ERK1/2 Abs (Cell Signaling Technology, Danvers, MA) at a 1:1000 dilution or with an anti-β actin Ab at a 1:2000 dilution overnight at 4˚C. After being washed with TBST three times, the membranes were incubated with a HRP-conjugated anti-rabbit IgG Ab (1:2000) for 1 h. The blots were washed again, and individual target proteins were visualized using an ECL detection system (Amersham Biosciences, Piscataway, NJ).

Real-time PCR

Quantitative real-time PCR was performed to measure the relative levels of cytokine and chemokine transcripts. Total RNA was extracted using the TRI reagent (Molecular Research Center, Cincinnati, OH) and reverse transcribed into cDNA using Moloney murine leukemia virus reverse transcriptase (Invitrogen, Carlsbad, CA) and gene-specific primers (Table I). Quantitative real-time PCR was performed using the ABI Prism 7700 System (PE Applied Biosystems, Foster City, CA). Finally, the measured expression levels were normalized to 18S rRNA and expressed as fold changes of the untreated controls.

ADAM-17 activity assay

Freshly isolated AEC I and AEC II from wild-type and $P2X_7R^{-/-}$ mice, with or without LPS plus MV treatment, or HEK-293 cells stably expressing the rat $P2X_7R$ (HEK-$P2X_7R$) and treated with BzATP (200 μM; Sigma-Aldrich) or the ERK1/2 inhibitor U0126 (10 μM; Promega, Madison, WI) for the indicated time periods were lysed. The lysate (25 μg) was analyzed for ADAM-17 activity using a fluorogenic peptide-based assay kit (R&D Systems). The enzymatic activity was obtained from a serially diluted standard of recombinant ADAM-17 run in parallel.

Zymography

Gelatin zymography was performed to evaluate the activities of MMP-2 and -9 in BAL fluids from wild-type and $P2X_7R^{-/-}$ mice. Ten micrograms

Table I. Real-time PCR primers

Gene	Forward Primer Sequences	Reverse Primer Sequences
mIL-1β	5′-GCAACTGTTCCTGAACTCAACT-3′	5′-ATCTTTTGGGGTCCGTCAACT-3′
mIL-6	5′-TAGTCCTTCCTACCCCAATTTCC-3′	5′-TTGGTCCTTAGCCACTCCTTC-3′
mMCP-1	5′-CTTCTGGGCCTGCTGTTCA-3′	5′-CCAGCCTACTCATTGGGATCA-3′
Rat IL-1β	5′-TTGCTTCCAAGCCCTTGACT-3′	5′-TGAGTGACACTGCCTTCCTGAA-3′
Rat IL-6	5′-CCACCAGGAACGAAAGTCAAC-3′	5′-TGTCAACAACATCAGTCCCAAGA-3′
18S	5′-ATTGCTCAATCTCGGGTGGCTG-3′	5′-CGTTCTTAGTTGGTGGAGCGATTTG-3′

mIL, murine IL; mMCP, murine MCP.

of protein from the BAL fluids was separated in an 8% SDS-polyacrylamide gel containing 0.2% gelatin. The gels were then washed and stained with Coomassie blue and destained with a mixture of acetic acid and methanol. The gels were finally scanned, and the band intensities were quantified (in arbitrary density units) using Image J software (National Institutes of Health). To eliminate differences between gels, two samples from all experimental groups were loaded in the same gel.

Statistical analysis

The results were analyzed using one-way ANOVA with Tukey's post hoc test for multiple comparisons of the control and treatment groups using GraphPad Prism software (version 4). All results are reported as the mean ± SE (n = 4–8). A difference was considered statistically significant when $p < 0.05$.

Results

Deficiency or antagonism of P2X$_7$R protects mice against acute lung injury

The patients with lung infections who develop ALI/ARDS are often placed on a mechanical ventilator. Thus, the two-hit murine low-dose LPS and moderate tidal volume MV-induced ALI model simulates the human situation more closely than other models (22). Employing this model, we examined whether the use of P2X$_7$R$^{-/-}$ mice or pharmacological inhibition of P2X$_7$R in wild-type mice would result in protection against LPS plus MV–induced lung injury. The neutrophil count in BAL fluid was increased by LPS plus MV treatment in wild-type mice ($7.0 \pm 1.0 \times 10^4$/ml BAL in LPS plus MV versus $0.04 \pm 0.007 \times 10^4$/ml BAL in control). The increase associated with LPS plus MV treatment was significantly smaller in P2X$_7$R$^{-/-}$ mice and AZ106006120 (P2X$_7$R inhibitor)-treated wild-type mice (Fig. 1A). The number of neutrophils in the BAL fluid was correlated with myeloperoxidase activity in the lung tissue, which is another indicator of neutrophil infiltration (Supplemental Fig. 1A). No appreciable difference in the number of macrophages in the BAL fluid was observed between wild-type and P2X$_7$R$^{-/-}$ mice (data not shown). The P2X$_7$R$^{-/-}$ and P2X$_7$R-inhibited mice showed reduced vascular permeability, as revealed based on EB dye extravasation (Fig. 1B) and/or BAL IgM levels (Fig. 1C). These mice also showed decreased levels of proinflammatory cytokines (IL-1β and IL-6) and a chemokine (MCP-1) in BAL following LPS plus MV treatment (Fig. 1D, 1E, Supplemental Fig. 1B). The mRNA induction of these cytokines in the lung tissues was 30–50% less in P2X$_7$R$^{-/-}$ mice compared with wild-type mice (Supplemental Fig. 1C–E).

In the LPS plus MV–challenged wild-type mice, diffuse lung injury with significant inflammatory cell infiltration around the interstitial, perivascular, and intra-alveolar spaces and a widespread infiltration of neutrophils within alveolar septa and lumens was observed (Fig. 1F, indicated by arrows). In contrast, P2X$_7$R$^{-/-}$ mice exhibited less neutrophil infiltration following LPS plus MV treatment (Fig. 1F, indicated by arrows). Numerous scattered foci of alveolar septal necrosis seen in wild-type mice (Fig. 1F, photo inset) were not observed in the lungs of P2X$_7$R$^{-/-}$ mice.

In a live *E. coli* infection mouse model, fewer neutrophils were observed in BAL fluid from P2X$_7$R$^{-/-}$ mice compared with wild-type mice. However, there was no difference in the amount of viable bacteria in unlavaged whole lungs between the P2X$_7$R$^{-/-}$ and wild-type mice (Supplemental Fig. 1F, 1G). Taken together, these results demonstrate that P2X$_7$R contributes to neutrophil infiltration, alveolar-endothelial barrier damage, and proinflammatory cytokine induction and release, but not to bacterial clearance in an ALI.

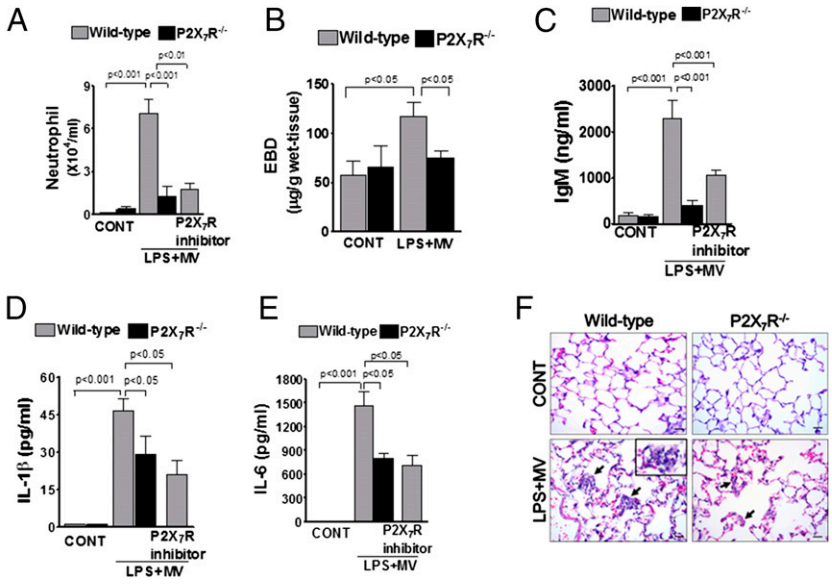

FIGURE 1. Reduced inflammation in mice associated with P2X$_7$R deficiency or antagonism during acute lung injury. Wild-type mice treated with or without a P2X$_7$R inhibitor (AZ10606120) and P2X$_7$R$^{-/-}$ mice were challenged with LPS plus mechanical ventilation (LPS + MV). (**A**) Neutrophils in BAL fluid, (**B**) EB dye extravasation, (**C**) IgM expression in BAL fluid, (**D**) IL-1β levels in BAL fluid, (**E**) IL-6 levels in BAL fluid, and (**F**) H&E staining. Arrows indicate alveolar septal necrosis. Scale bar, 50 μm. Data are expressed as the mean ± SE (n = 4–8).

Soluble VCAM-1 functions as a novel chemoattractant for neutrophils

To identify the cytokines responsible for the observed differences in neutrophil recruitment between wild-type and $P2X_7R^{-/-}$ mice, we performed a cytokine Ab array analysis of BAL fluids from wild-type and $P2X_7R^{-/-}$ mice following LPS plus MV challenge. Among the 144 cytokines assessed, including chemokines and other soluble mediators, we detected 54 cytokines in BAL fluids. Of these cytokines, 34 were induced by LPS plus MV treatment, in which 25 showed no significant differences between wild-type and $P2X_7R^{-/-}$ mice, and 9 cytokines showed less induction by LPS plus MV treatment in $P2X_7R^{-/-}$ mice (Supplemental Fig. 2A, 2B, Supplemental Table I). The changes in IL-6 and MCP-1 levels revealed by the cytokine array were consistent with the ELISA results (Fig. 1E, Supplemental Fig. 1B). IL-1β was not detected by the Ab array due to its low expression level. We noted that the BAL levels of the known neutrophil chemokines, keratinocyte-derived chemokine (IL-8 or CINC-1), MIP-2, LIX, and lungkine (9, 26–29), were not different between wild-type and $P2X_7R^{-/-}$ mice challenged with LPS and MV (Supplemental Table I). This suggests that an unknown chemokine/chemoattractant (s) is responsible for recruiting excess neutrophils to the lungs in our ALI model. Unexpectedly, the expression level of sVCAM-1 in BAL fluid was increased by LPS plus MV treatment in wild-type mice and, to a lesser extent, in $P2X_7R^{-/-}$ mice (Supplemental Fig. 2B). This result was confirmed via ELISA (Fig. 2A). The sVCAM-1 level was also reduced following $P2X_7R$ antagonism.

VCAM-1, a type I transmembrane protein of the Ig superfamily, mediates the rolling and adherence of monocytes, lymphocytes, and eosinophils via the $\alpha_4\beta_1$ integrin in the vasculature (30) and has been implicated in asthma (31). Induction of β_1 integrin in neutrophils has been reported under pathological conditions (14, 15, 32). As the first step to elucidate the function of sVCAM-1 in neutrophil recruitment, we first determined whether the integrins responsible for VCAM-1 binding were induced in neutrophils, including $\alpha_4\beta_1$ (VLA-4, CD49d/CD29), $\alpha_4\beta_7$ (LPAM-1, CD49d/CD103), and $\alpha_M\beta_2$ (CD11b/CD18). LPS plus MV treatment increased the expression levels of the α_4, β_7, and α_M integrins in BAL neutrophils from both wild-type and $P2X_7R^{-/-}$ mice (Fig. 2B–D). Isotype control Ab (rat IgG2b, κ) staining yielded little fluorescence (data not shown). It was noted that LPS plus MV treatment also upregulated α_4, but not β_7 or α_M integrin in circulating blood neutrophils. However, there were no differences in the expression of these integrins on circulating and BAL neutrophils detected between wild-type and $P2X_7R^{-/-}$ mice, suggesting that the observed difference in neutrophil recruitment between wild-type and $P2X_7R^{-/-}$ mice was not due to the rolling and adherence of neutrophils.

We then performed a chemotaxis assay (33) and found that recombinant sVCAM-1 showed chemotactic activity toward peripheral activated neutrophils in which the number of integrin receptors was maximized via cytochalasin treatment (34) (Fig. 2E). The neutrophils isolated from bone marrow have been shown to

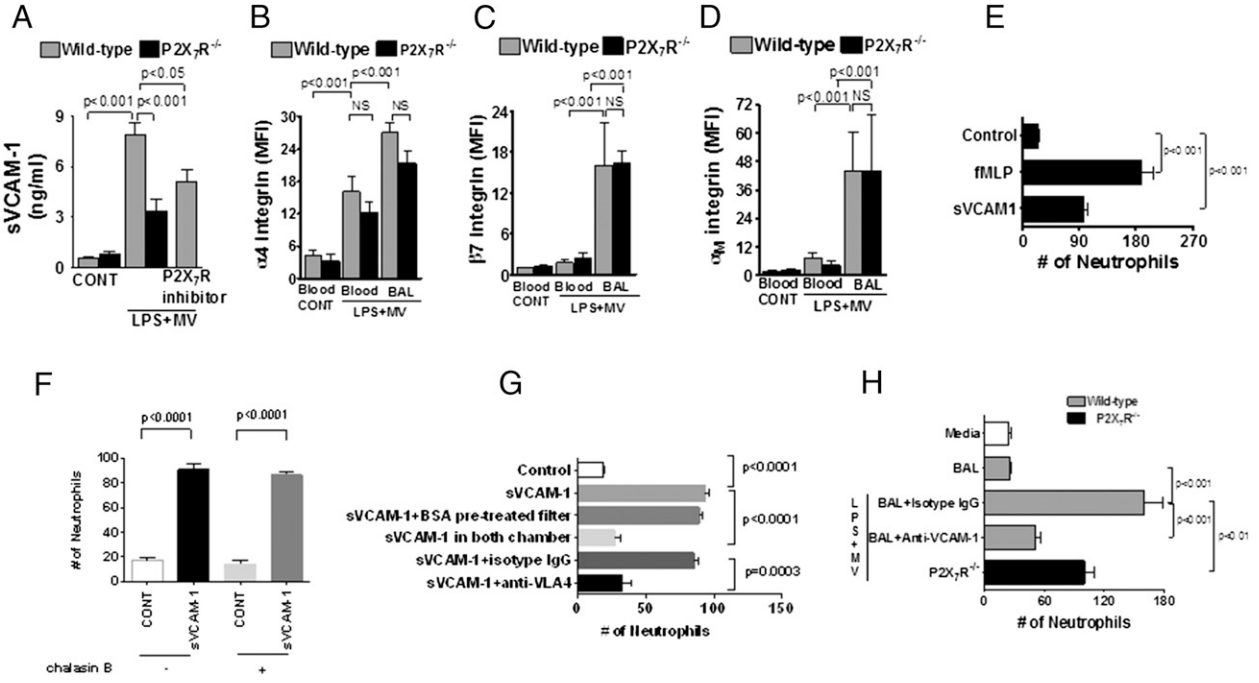

FIGURE 2. Alveolar sVCAM-1 induces neutrophil chemotaxis. (**A**) sVCAM-1 levels in BAL fluids from wild-type and $P2X_7R^{-/-}$ mice with or without $P2X_7R$ inhibition, following LPS plus MV challenge. Each data point from the individual animals was measured in duplicate, and the averages are expressed as the mean ± SE (n = 5–8 animals). (**B**) α_4, (**C**) β_7, and (**D**) α_M integrin expression in circulating or infiltrated neutrophils in BAL fluids from wild-type and $P2X_7R^{-/-}$ mice following the LPS plus MV challenge, determined in flow cytometric analyses. The fluorescence intensity was measured from 5000 Gr-1–positive cells. The background labeled with the isotype control Ab was subtracted from the mean fluorescence intensities (MFI). (n = 4 animals.) (**E**–**H**) Chemotaxis assays. Neutrophils were added to the upper chamber and sVCAM (10 μg/ml) or other chemoattractants were placed in the lower chamber. The cells that migrated and adhered to the lower surface of the membrane were counted from 10 microscopic fields under original magnification ×40. Data are expressed as the mean ± SE from three independent preparations, assayed in duplicate. (E) Upper chamber: dihydrochalasin B–treated rat peripheral neutrophils, and lower chamber: murine sVCAM-1 or fMLP (100 μM, a positive control). (F) Upper chamber: mouse bone marrow neutrophils with or without dihydrochalasin B treatment, and lower chamber: sVCAM-1. (G) Upper chamber: dihydrochalasin B–treated mouse bone marrow neutrophils, and lower chamber: sVCAM-1 or sVCAM-1 plus isotype IgG or anti-VLA4 Abs (Pierce integrin α_4/CD49d Ab, HP2/1, 1-h preincubation). In one experiment, the same amounts of sVCAM-1 were added to both upper and lower chambers. In another experiment, the filter membrane was pretreated with BSA. (H) Upper chamber: dihydrochalasin B–treated rat peripheral neutrophils, and lower chamber: control media or BAL fluid from control and LPS plus MV–challenged wild-type or $P2X_7R^{-/-}$ mice with an anti–VCAM-1 Ab or an isotype control IgG Ab.

express a high level of endogenous VLA-4 ($\alpha_4\beta_1$ integrin) compared with the circulating neutrophils (35). To eliminate the possible nonspecific effects of cytochalasin treatment, we tested whether sVCAM-1 had chemotactic activity toward bone marrow neutrophils. Indeed, sVCAM-1 increased the migration of untreated bone marrow neutrophils, and cytochalasin treatment had no significant effects on the chemotactic activity (Fig. 2F). We also performed checkerboard assay (36), in which sVCAM-1 was placed in both lower and upper chamber. In this assay, chemotactic activity of sVCAM-1 was eliminated (Fig. 2G). In addition, the pretreatment of the filter membrane with BSA had no effects on sVCAM-1–mediated neutrophil migration, suggesting that the observed effects were not due to sVCAM-1 absorption to the filter membrane. Furthermore, anti–VLA-4 Ab blocked sVCAM-1–mediated neutrophil migration. All of the results suggest that sVCAM-1 induces directional migration.

BAL fluid from LPS plus MV–challenged mice also exhibited chemotactic activity, which was blocked by anti–VCAM-1 Abs. Furthermore, BAL fluid from LPS plus MV–treated $P2X_7R^{-/-}$ mice showed lower neutrophil chemotactic activity (Fig. 2H).

To determine whether sVCAM-1 is responsible for neutrophil recruitment in vivo, we neutralized VCAM-1 in the alveoli using an anti–VCAM-1 Ab. Intratracheal blockade of VCAM-1 yielded a striking decrease in the number of BAL neutrophils (Fig. 3A). However, there was no significant difference in macrophage recruitment observed following treatment (data not shown). The release of IL-1β and IL-6 into the alveolar space was also reduced by VCAM-1 blockade (Fig. 3B, 3C).

To directly demonstrate that the reduced neutrophil infiltration observed in $P2X_7R^{-/-}$ mice challenged with LPS plus MV was due to sVCAM-1, we performed a rescue experiment in $P2X_7R^{-/-}$ mice. The administration of sVCAM-1 in the lungs of $P2X_7R^{-/-}$ mice restored lung neutrophil infiltration following a LPS plus MV challenge (Fig. 3D). BAL IL-1β and IL-6 levels were also increased by the administration of sVCAM-1 to $P2X_7R^{-/-}$ mice (Fig. 3E, 3F). Our results suggest that the neutrophil infiltration observed in the wild-type mice following LPS plus MV treatment is a consequence of increased sVCAM-1 levels in BAL and is $P2X_7R$ dependent.

Soluble VCAM-1 activates alveolar macrophages

We further investigated whether sVCAM-1 could activate alveolar macrophages and thus amplify inflammation. sVCAM-1 bound to rat alveolar macrophages in a concentration-dependent manner, as determined through cell-based ELISA (Fig. 4A). sVCAM-1 increased nitrate/nitrite production (Fig. 4B) and induced the expression of IL-1β and IL-6 mRNA in alveolar macrophages (Fig. 4C, 4D), suggesting that sVCAM-1 activates alveolar macrophages and potentially intensifies the inflammatory response through enhanced cytokine induction.

Soluble VCAM-1 is shed from AEC I and requires $P2X_7R$

The marked increase of sVCAM-1 observed in the alveolar airspace during ALI suggests that alveolar epithelial cells may be involved in VCAM-1 shedding. To identify which types of cells express VCAM-1 in the alveolar epithelium, mouse AEC II were *trans*-differentiated into AEC I via 5 d of culture (37). VCAM-1 was expressed in AEC I, but not in AEC II or alveolar macrophages (Fig. 5A, Supplemental Fig. 3A). We then isolated primary alveolar epithelial cells (a 1:2 ratio of AEC I and AEC II cell mixture) from LPS plus MV–challenged wild-type and $P2X_7R^{-/-}$ mice using a protocol we have described previously (21). Flow cytometric analysis of freshly isolated alveolar epithelial cells

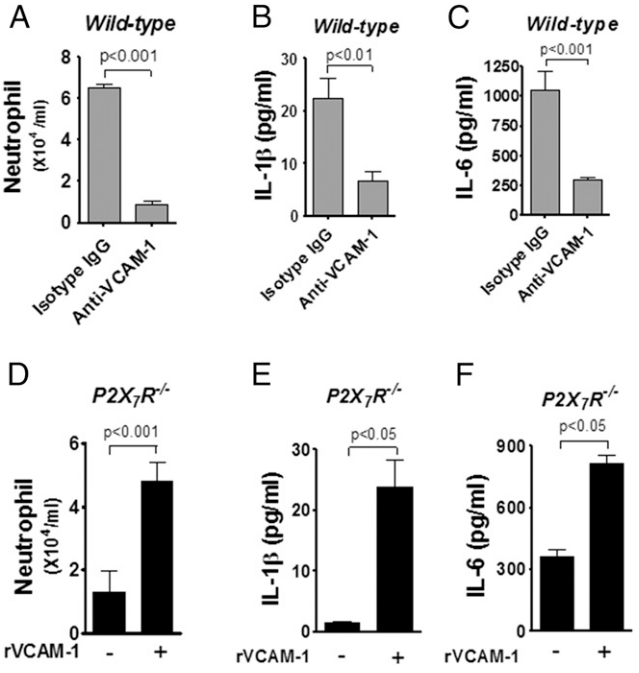

FIGURE 3. Effects of Abs blocking VCAM-1 function in wild-type mice and sVCAM-1 reconstitution in $P2X_7R^{-/-}$ mice on acute pulmonary inflammation. Wild-type or $P2X_7R^{-/-}$ mice were intratracheally coadministered LPS with an isotype-matched control IgG Ab and function-blocking mAbs against VCAM-1 (88 μg/mouse) or murine recombinant VCAM-1 (5 μg/mouse), followed by mechanical ventilation. Neutrophil counts (**A** and **D**), IL-1β levels (**B** and **E**), and IL-6 levels (**C** and **F**) in BAL fluid. Values are given as the mean ± SE (n = 5–8 animals).

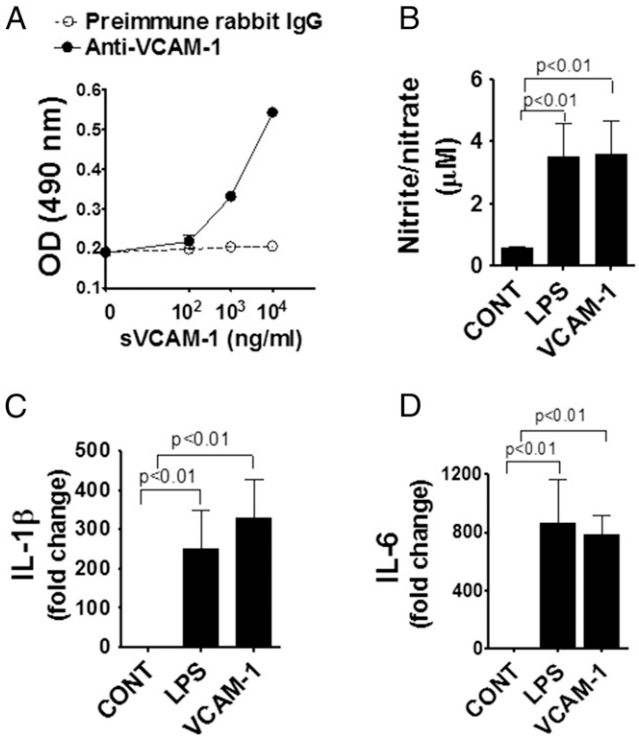

FIGURE 4. sVCAM-1 activates alveolar macrophages. (**A**) The binding of sVCAM-1 to alveolar macrophages, as determined by a cell-based ELISA. Rat alveolar macrophages were incubated with sVCAM-1, followed by incubation with anti–VCAM-1 Abs or a control IgG Ab, and quantification was performed based on the OD. (**B**–**D**) Concentrations of nitrite and nitrate in the media and IL-1β and IL-6 mRNA levels in rat alveolar macrophages stimulated with LPS (1 μg/ml) and VCAM-1 (10 μg/ml) for 4 h (n = 4).

indicated that the cell surface expression of VCAM-1 in AEC I (T1α-positive cells) was increased by LPS plus MV treatment in wild-type mice, and the observed induction was less in $P2X_7R^{-/-}$ mice (Fig. 5B). In vitro treatment with IL-1β increased VCAM-1 protein levels in AEC I from wild-type mice, but not in those from $P2X_7R^{-/-}$ mice (Fig. 5C). IL-1β also stimulated the shedding of VCAM-1 from wild-type AEC I in a dose-dependent manner, and this effect was not observed in AEC I from $P2X_7R^{-/-}$ mice (Fig. 5D). Functionally, conditioned media from IL-1β–treated wild-type, but not $P2X_7R^{-/-}$ AEC I increased the migration of neutrophils (Fig. 5E). These data suggest that sVCAM-1 is shed from AEC I in a $P2X_7R$-dependent manner.

Soluble VCAM-1 shedding from the surface of AEC I occurs through ADAM-17

ADAM-17 has been shown to cleave VCAM-1 in stomach epithelial cells (38). ADAM-17 was highly expressed in AEC I, but showed a very low level of expression in AEC II (Fig. 6A). The ADAM-17 activity determined with a fluorogenic peptide based-assay kit in primary alveolar epithelial cells from LPS plus MV–treated wild-type mice was increased compared with LPS plus MV–treated $P2X_7R^{-/-}$ mice (Fig. 6B). However, ADAM-17 mRNA expression was not induced by LPS plus MV treatment (data not shown). The MMP-2 and MMP-9 activities detected in BAL fluids from wild-type and $P2X_7R^{-/-}$ mice were similar following LPS plus MV treatment, as demonstrated via gelatin zymography (Supplemental Fig. 2C, 2D). GM-6001, a broad inhibitor of the MMP and ADAM families, inhibited sVCAM-1 release from the IL-1β–treated AEC I (Fig. 6C). Silencing of ADAM-17 using a lentiviral shRNA also reduced IL-1β–induced sVCAM-1 shedding from AEC I (Fig. 6D).

$P2X_7R$ activates ERK in various cell types (39, 40), and ERK phosphorylates ADAM-17 (41). We therefore examined whether the ERK pathway was activated in AEC I stimulated with BzATP, an agonist of $P2X_7R$. A striking increase in the phosphorylation of P42/44, but not in the total amount of P42/44, was observed after BzATP stimulation (Fig. 6E). Furthermore, BzATP stimulation increased ADAM-17 activity, which was blocked by the ERK-1/2 inhibitor U0126 (Fig. 6F, Supplemental Fig. 3B). Collectively, these results support the hypothesis that VCAM-1 shedding from AEC I is mediated by ADAM-17 activation through the $P2X_7R$-stimulated ERK pathway.

Discussion

VCAM-1 was originally identified as a cytokine-inducible adhesion molecule on human endothelial cells (42, 43). The membrane-bound form of VCAM-1 is found on the surface of leukocytes and acts as a ligand for the $\alpha_4\beta_1$ and $\alpha_4\beta_7$ integrins (15, 44, 45). VCAM-1 mediates the transmigration of α_4 integrin–positive cells across the inflamed endothelium and epithelium of the lungs (46, 47). VCAM-1 can be released as a soluble variant, sVCAM-1, via proteolytic cleavage (38). sVCAM-1 binds with $\alpha_4\beta_1$ integrins and alters lymphocyte functions and angiogenesis (48, 49). sVCAM-1 levels are elevated in biological fluids in various diseases, including synovial fluids from patients with rheumatoid arthritis (50), cerebrospinal fluid from patients with active multiple sclerosis (51), and alveolar lining fluid from patients with eosinophilic pneumonia and asthma (52). However, the physiological functions of sVCAM-1 are unknown.

The early migration of circulating neutrophils into the airspaces involves the adhesion of neutrophils to endothelial cells. This process is mediated by β_2 integrin–dependent and –independent mechanisms. In various mouse models of lung injury, neutrophil infiltration is significantly reduced in mice treated with anti–ICAM-1 or anti-β_2 integrin Abs (53–55). The β_2 integrin–independent neutrophil influx also plays an important role during bacterial pneumonia (11, 56). The association of the α_4 integrin on activated neutrophils with its VCAM-1 substrate increases rolling and adherence, independent of selectins and β_2 integrins (14, 15). The shear forces in pulmonary capillaries are weak, but sufficient to support $\alpha_4\beta_1$ integrin–mediated tethering and adhesion interactions (14). Based on the induction of α_4 integrin expression observed on circulating neutrophils during ALI, VCAM-1 expression on endothelial cells could be an additional mechanism for neutrophil adhesion to the endothelium for excess neutrophil recruitment. However, there was no difference in neutrophil-surface β_1 integrin expression detected between wild-type and $P2X_7R^{-/-}$

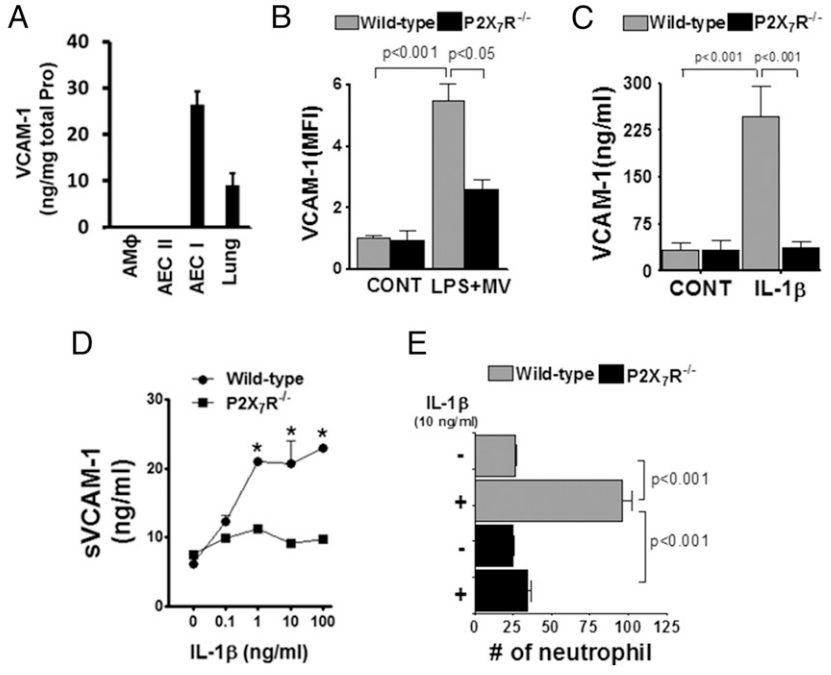

FIGURE 5. VCAM-1 is shed from alveolar epithelial type I cells in a $P2X_7R$-dependent manner. (**A**) ELISA analysis of VCAM-1 expression in mouse alveolar macrophages (AMϕ), alveolar epithelial type II cells (AEC II), type I cells *trans*-differentiated from type II cells (AEC I), and lung tissue ($n = 3$). (**B**) FACS analysis of cell surface VCAM-1 expression in podoplanin (AEC I marker)-positive cells. (**C**) ELISA analysis of VCAM-1 expression in AEC I from wild-type and $P2X_7R^{-/-}$ mice treated with IL-1β (10 ng/ml). (**D**) Dose response of sVCAM-1 shedding in IL-1β–stimulated AEC I, for 48 h. (**E**) Migration of neutrophils toward 50% conditioned media collected from IL-1β (10 ng/ml)–treated AEC I. All data are expressed as the mean ± SE. Three independent cell preparations were used. $*p < 0.05$ versus control (0 IL-1β).

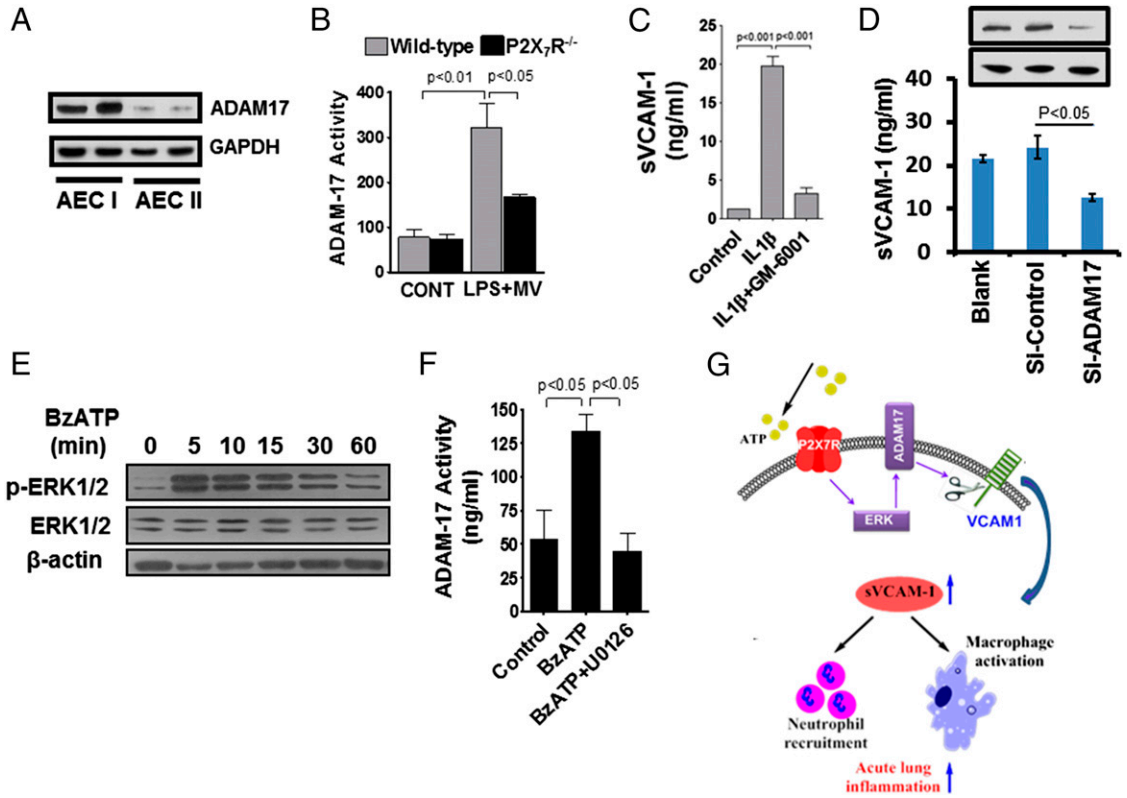

FIGURE 6. VCAM-1 shedding is mediated by ADAM-17. (**A**) Western blot analysis of ADAM-17 expression in mouse alveolar epithelial type II cells (AEC II) and AEC I *trans*-differentiated from AEC II. (**B**) ADAM-17 activity in freshly isolated AEC from control (CONT) and LPS plus MV–challenged mice ($n = 3$). (**C**) Inhibition of VCAM-1 shedding by the ADAM inhibitor GM-6001 in IL-1β–treated AEC I ($n = 3$). (**D**) Effect of ADAM-17 silencing on ADAM-17 protein levels and IL-1β–induced sVCAM-1 release from mouse AEC I ($n = 3$). Si-Control: lentivirus control with a scrambled sequence. Si-ADAM-17: lentivirus with a small interfering RNA targeting ADAM-17. Multiplicity of infection = 100. (**E**) ERK1/2 phosphorylation in an AEC I cell line, E10, stimulated with the $P2X_7R$ agonist BzATP. (**F**) ADAM-17 activity in HEK cells stably expressing $P2X_7R$ with BzATP stimulation and ERK1/2 inhibition with U0126. (**G**) A model of sVCAM-1–mediated acute pulmonary inflammation.

mice. Thus, this mechanism is most likely not a major contributor in the observed $P2X_7R^{-/-}$ phenotype.

The high level of BAL sVCAM-1 observed in the LPS plus MV–treated ALI model suggests a possible pathophysiological role for sVCAM-1 in lung injury. Functional blockade of alveolar VCAM-1 activity was found to be protective in our model of acute lung injury, as demonstrated by the reduced neutrophil infiltration and IL-1β and IL-6 production detected in BAL fluid. These results could indicate two new functions of sVCAM-1: as a neutrophil chemoattractant and a macrophage activator.

VCAM-1 ectodomain shedding has been reported in activated endothelial cells and contributes to the amount of circulating VCAM-1 (57, 58). In this study, to our knowledge, we show for the first time that VCAM-1 is shed from AEC I during ALI, constituting a major source of sVCAM-1 in alveoli. VCAM-1 was highly expressed in AEC I, but not in AEC II or alveolar macrophages. The inflammatory cytokine IL-1β stimulated sVCAM-1 release from AEC I in cell culture and during ALI. This finding is consistent with the reported induction of VCAM-1 in bronchial epithelial cells in response to acute lung injury (59) and shedding of VCAM-1 from the inflamed epithelia (60). VCAM-1 shedding can be mediated by disintegrin and metalloprotease family (38, 57, 58). Neutrophil proteases including elastase and cathepsin G have been shown to cleave VCAM-1 in bone marrow stromal cells (61). Several lines of evidence support the hypothesis that the activation of $P2X_7R$ is coupled with ADAM-17–induced sVCAM-1 generation from AEC I through the ERK pathway: 1) all three proteins ($P2X_7R$, ADAM-17, and sVCAM-1) were highly expressed in AEC I; 2) ADAM-17 activity was increased in AEC I isolated from LPS plus MV–challenged $P2X_7R^{-/-}$ mice to a lesser degree than in those from wild-type mice; 3) VCAM-1 shedding was increased by IL-1β, which was blocked by a metalloproteinase inhibitor; 4) knockdown of ADAM-17 reduced VCAM-1 shedding; and 5) treatment with BzATP, an agonist of $P2X_7R$, stimulated the ERK pathway and increased the enzymatic activity of ADAM-17 in AEC I, which was blocked with an ERK inhibitor.

In summary, we report a novel mechanism by which $P2X_7R$ on AEC I regulates the shedding of VCAM-1, which functions as a neutrophil chemoattractant and a macrophage activator to recruit pathological neutrophils through β_1 integrins.

Disclosures

The authors have no financial conflicts of interest.

References

1. Matthay, M. A., and R. L. Zemans. 2011. The acute respiratory distress syndrome: pathogenesis and treatment. *Annu. Rev. Pathol.* 6: 147–163.
2. Balamayooran, G., S. Batra, M. B. Fessler, K. I. Happel, and S. Jeyaseelan. 2010. Mechanisms of neutrophil accumulation in the lungs against bacteria. *Am. J. Respir. Cell Mol. Biol.* 43: 5–16.
3. Martin, T. R., B. P. Pistorese, E. Y. Chi, R. B. Goodman, and M. A. Matthay. 1989. Effects of leukotriene B4 in the human lung: recruitment of neutrophils into the alveolar spaces without a change in protein permeability. *J. Clin. Invest.* 84: 1609–1619.
4. Ong, E. S., X. P. Gao, N. Xu, D. Predescu, A. Rahman, M. T. Broman, D. H. Jho, and A. B. Malik. 2003. *E. coli* pneumonia induces CD18-independent airway neutrophil migration in the absence of increased lung vascular permeability. *Am. J. Physiol. Lung Cell. Mol. Physiol.* 285: L879–L888.

5. Tateda, K., T. A. Moore, J. C. Deng, M. W. Newstead, X. Zeng, A. Matsukawa, M. S. Swanson, K. Yamaguchi, and T. J. Standiford. 2001. Early recruitment of neutrophils determines subsequent T1/T2 host responses in a murine model of *Legionella pneumophila* pneumonia. *J. Immunol.* 166: 3355–3361.
6. Jeyaseelan, S., S. K. Young, M. Yamamoto, P. G. Arndt, S. Akira, J. K. Kolls, and G. S. Worthen. 2006. Toll/IL-1R domain-containing adaptor protein (TIRAP) is a critical mediator of antibacterial defense in the lung against *Klebsiella pneumoniae* but not *Pseudomonas aeruginosa. J. Immunol.* 177: 538–547.
7. Abraham, E., A. Carmody, R. Shenkar, and J. Arcaroli. 2000. Neutrophils as early immunologic effectors in hemorrhage- or endotoxemia-induced acute lung injury. *Am. J. Physiol. Lung Cell. Mol. Physiol.* 279: L1137–L1145.
8. Chen, S. C., B. Mehrad, J. C. Deng, G. Vassileva, D. J. Manfra, D. N. Cook, M. T. Wiekowski, A. Zlotnik, T. J. Standiford, and S. A. Lira. 2001. Impaired pulmonary host defense in mice lacking expression of the CXC chemokine lungkine. *J. Immunol.* 166: 3362–3368.
9. Jeyaseelan, S., R. Manzer, S. K. Young, M. Yamamoto, S. Akira, R. J. Mason, and G. S. Worthen. 2005. Induction of CXCL5 during inflammation in the rodent lung involves activation of alveolar epithelium. *Am. J. Respir. Cell Mol. Biol.* 32: 531–539.
10. Snelgrove, R. J., P. L. Jackson, M. T. Hardison, B. D. Noerager, A. Kinloch, A. Gaggar, S. Shastry, S. M. Rowe, Y. M. Shim, T. Hussell, and J. E. Blalock. 2010. A critical role for LTA4H in limiting chronic pulmonary neutrophilic inflammation. *Science* 330: 90–94.
11. Kumasaka, T., N. A. Doyle, W. M. Quinlan, L. Graham, and C. M. Doerschuk. 1996. Role of CD11/CD18 in neutrophil emigration during acute and recurrent *Pseudomonas aeruginosa*-induced pneumonia in rabbits. *Am. J. Pathol.* 148: 1297–1305.
12. Bowden, R. A., Z. M. Ding, E. M. Donnachie, T. K. Petersen, L. H. Michael, C. M. Ballantyne, and A. R. Burns. 2002. Role of alpha4 integrin and VCAM-1 in CD18-independent neutrophil migration across mouse cardiac endothelium. *Circ. Res.* 90: 562–569.
13. Burns, J. A., T. B. Issekutz, H. Yagita, and A. C. Issekutz. 2001. The alpha 4 beta 1 (very late antigen (VLA)-4, CD49d/CD29) and alpha 5 beta 1 (VLA-5, CD49e/CD29) integrins mediate beta 2 (CD11/CD18) integrin-independent neutrophil recruitment to endotoxin-induced lung inflammation. *J. Immunol.* 166: 4644–4649.
14. Reinhardt, P. H., J. F. Elliott, and P. Kubes. 1997. Neutrophils can adhere via alpha4beta1-integrin under flow conditions. *Blood* 89: 3837–3846.
15. Ibbotson, G. C., C. Doig, J. Kaur, V. Gill, L. Ostrovsky, T. Fairhead, and P. Kubes. 2001. Functional alpha4-integrin: a newly identified pathway of neutrophil recruitment in critically ill septic patients. *Nat. Med.* 7: 465–470.
16. Lucattelli, M., S. Cicko, T. Müller, M. Lommatzsch, G. De Cunto, S. Cardini, W. Sundas, M. Grimm, R. Zeiser, T. Dürk, et al. 2011. P2X7 receptor signaling in the pathogenesis of smoke-induced lung inflammation and emphysema. *Am. J. Respir. Cell Mol. Biol.* 44: 423–429.
17. Muller, T., V. R. Paula, M. Grimm, T. Durk, S. Cicko, R. Zeiser, T. Jakob, S. F. Martin, B. Blumenthal, S. Sorichter, et al. 2010. A potential role for P2X7R in allergic airway inflammation in mice and humans. *Am. J. Respir. Cell Mol. Biol.* 44: 456–464.
18. Riteau, N., P. Gasse, L. Fauconnier, A. Gombault, M. Couegnat, L. Fick, J. Kanellopoulos, V. F. Quesniaux, S. Marchand-Adam, B. Crestani, et al. 2010. Extracellular ATP is a danger signal activating P2X7 receptor in lung inflammation and fibrosis. *Am. J. Respir. Crit. Care Med.* 182: 774–783.
19. Denlinger, L. C., L. Shi, A. Guadarrama, K. Schell, D. Green, A. Morrin, K. Hogan, R. L. Sorkness, W. W. Busse, and J. E. Gern. 2009. Attenuated P2X7 pore function as a risk factor for virus-induced loss of asthma control. *Am. J. Respir. Crit. Care Med.* 179: 265–270.
20. Chen, Z., N. Jin, T. Narasaraju, J. Chen, L. R. McFarland, M. Scott, and L. Liu. 2004. Identification of two novel markers for alveolar epithelial type I and II cells. *Biochem. Biophys. Res. Commun.* 319: 774–780.
21. Mishra, A., N. R. Chintagari, Y. Guo, T. Weng, L. Su, and L. Liu. 2011. Purinergic P2X7 receptor regulates lung surfactant secretion in a paracrine manner. *J. Cell Sci.* 124: 657–668.
22. Altemeier, W. A., G. Matute-Bello, S. A. Gharib, R. W. Glenny, T. R. Martin, and W. C. Liles. 2005. Modulation of lipopolysaccharide-induced gene transcription and promotion of lung injury by mechanical ventilation. *J. Immunol.* 175: 3369–3376.
23. Narasaraju, T. A., N. Jin, C. R. Narendranath, Z. Chen, D. Gou, and L. Liu. 2003. Protein nitration in rat lungs during hyperoxia exposure: a possible role of myeloperoxidase. *Am. J. Physiol. Lung Cell. Mol. Physiol.* 285: L1037–L1045.
24. Chen, J., Z. Chen, N. R. Chintagari, M. Bhaskaran, N. Jin, T. Narasaraju, and L. Liu. 2006. Alveolar type I cells protect rat lung epithelium from oxidative injury. *J. Physiol.* 572: 625–638.
25. Corti, M., A. R. Brody, and J. H. Harrison. 1996. Isolation and primary culture of murine alveolar type II cells. *Am. J. Respir. Cell Mol. Biol.* 14: 309–315.
26. Manzer, R., J. Wang, K. Nishina, G. McConville, and R. J. Mason. 2006. Alveolar epithelial cells secrete chemokines in response to IL-1beta and lipopolysaccharide but not to ozone. *Am. J. Respir. Cell Mol. Biol.* 34: 158–166.
27. Witherden, I. R., E. J. Vanden Bon, P. Goldstraw, C. Ratcliffe, U. Pastorino, and T. D. Tetley. 2004. Primary human alveolar type II epithelial cell chemokine release: effects of cigarette smoke and neutrophil elastase. *Am. J. Respir. Cell Mol. Biol.* 30: 500–509.
28. Thorley, A. J., P. A. Ford, M. A. Giembycz, P. Goldstraw, A. Young, and T. D. Tetley. 2007. Differential regulation of cytokine release and leukocyte migration by lipopolysaccharide-stimulated primary human lung alveolar type II epithelial cells and macrophages. *J. Immunol.* 178: 463–473.
29. Vanderbilt, J. N., E. M. Mager, L. Allen, T. Sawa, J. Wiener-Kronish, R. Gonzalez, and L. G. Dobbs. 2003. CXC chemokines and their receptors are expressed in type II cells and upregulated following lung injury. *Am. J. Respir. Cell Mol. Biol.* 29: 661–668.
30. Cook-Mills, J. M., M. E. Marchese, and H. Abdala-Valencia. 2011. Vascular cell adhesion molecule-1 expression and signaling during disease: regulation by reactive oxygen species and antioxidants. *Antioxid. Redox Signal.* 15: 1607–1638.
31. Gonzalo, J. A., C. M. Lloyd, L. Kremer, E. Finger, C. Martinez-A, M. H. Siegelman, M. Cybulsky, and J. C. Gutierrez-Ramos. 1996. Eosinophil recruitment to the lung in a murine model of allergic inflammation: the role of T cells, chemokines, and adhesion receptors. *J. Clin. Invest.* 98: 2332–2345.
32. Guo, R. F., N. C. Riedemann, I. J. Laudes, V. J. Sarma, R. G. Kunkel, K. A. Dilley, J. D. Paulauskis, and P. A. Ward. 2002. Altered neutrophil trafficking during sepsis. *J. Immunol.* 169: 307–314.
33. Ueki, S., J. Kihara, H. Kato, W. Ito, M. Takeda, Y. Kobayashi, H. Kayaba, and J. Chihara. 2009. Soluble vascular cell adhesion molecule-1 induces human eosinophil migration. *Allergy* 64: 718–724.
34. Kubes, P., X. F. Niu, C. W. Smith, M. E. Kehrli, Jr., P. H. Reinhardt, and R. C. Woodman. 1995. A novel beta 1-dependent adhesion pathway on neutrophils: a mechanism invoked by dihydrocytochalasin B or endothelial transmigration. *FASEB J.* 9: 1103–1111.
35. Petty, J. M., C. C. Lenox, D. J. Weiss, M. E. Poynter, and B. T. Suratt. 2009. Crosstalk between CXCR4/stromal derived factor-1 and VLA-4/VCAM-1 pathways regulates neutrophil retention in the bone marrow. *J. Immunol.* 182: 604–612.
36. Kitani, A., N. Nakashima, T. Izumihara, M. Inagaki, X. Baoui, S. Yu, T. Matsuda, and T. Matsuyama. 1998. Soluble VCAM-1 induces chemotaxis of Jurkat and synovial fluid T cells bearing high affinity very late antigen-4. *J. Immunol.* 161: 4931–4938.
37. Bhaskaran, M., N. Kolliputi, Y. Wang, D. Gou, N. R. Chintagari, and L. Liu. 2007. Trans-differentiation of alveolar epithelial type II cells to type I cells involves autocrine signaling by transforming growth factor beta 1 through the Smad pathway. *J. Biol. Chem.* 282: 3968–3976.
38. Garton, K. J., P. J. Gough, J. Philalay, P. T. Wille, C. P. Blobel, R. H. Whitehead, P. J. Dempsey, and E. W. Raines. 2003. Stimulated shedding of vascular cell adhesion molecule 1 (VCAM-1) is mediated by tumor necrosis factor-alpha-converting enzyme (ADAM 17). *J. Biol. Chem.* 278: 37459–37464.
39. Budagian, V., E. Bulanova, L. Brovko, Z. Orinska, R. Fayad, R. Paus, and S. Bulfone-Paus. 2003. Signaling through P2X7 receptor in human T cells involves p56lck, MAP kinases, and transcription factors AP-1 and NF-kappa B. *J. Biol. Chem.* 278: 1549–1560.
40. Gendron, F. P., J. T. Neary, P. M. Theiss, G. Y. Sun, F. A. Gonzalez, and G. A. Weisman. 2003. Mechanisms of P2X7 receptor-mediated ERK1/2 phosphorylation in human astrocytoma cells. *Am. J. Physiol. Cell Physiol.* 284: C571–C581.
41. Soond, S. M., B. Everson, D. W. Riches, and G. Murphy. 2005. ERK-mediated phosphorylation of Thr735 in TNFalpha-converting enzyme and its potential role in TACE protein trafficking. *J. Cell Sci.* 118: 2371–2380.
42. Osborn, L., C. Hession, R. Tizard, C. Vassallo, S. Luhowskyj, G. Chi-Rosso, and R. Lobb. 1989. Direct expression cloning of vascular cell adhesion molecule 1, a cytokine-induced endothelial protein that binds to lymphocytes. *Cell* 59: 1203–1211.
43. Rice, G. E., and M. P. Bevilacqua. 1989. An inducible endothelial cell surface glycoprotein mediates melanoma adhesion. *Science* 246: 1303–1306.
44. Elices, M. J., L. Osborn, Y. Takada, C. Crouse, S. Luhowskyj, M. E. Hemler, and R. R. Lobb. 1990. VCAM-1 on activated endothelium interacts with the leukocyte integrin VLA-4 at a site distinct from the VLA-4/fibronectin binding site. *Cell* 60: 577–584.
45. Rüegg, C., A. A. Postigo, E. E. Sikorski, E. C. Butcher, R. Pytela, and D. J. Erle. 1992. Role of integrin alpha 4 beta 7/alpha 4 beta P in lymphocyte adherence to fibronectin and VCAM-1 and in homotypic cell clustering. *J. Cell Biol.* 117: 179–189.
46. Chin, J. E., C. A. Hatfield, G. E. Winterrowd, J. R. Brashler, S. L. Vonderfecht, S. F. Fidler, R. L. Griffin, K. P. Kolbasa, R. F. Krzesicki, L. M. Sly, et al. 1997. Airway recruitment of leukocytes in mice is dependent on alpha4-integrins and vascular cell adhesion molecule-1. *Am. J. Physiol.* 272: L219–L229.
47. Parmley, L. A., N. D. Elkins, M. A. Fini, Y. E. Liu, J. E. Repine, and R. M. Wright. 2007. Alpha-4/beta-1 and alpha-L/beta-2 integrins mediate cytokine induced lung leukocyte-epithelial adhesion and injury. *Br. J. Pharmacol.* 152: 915–929.
48. Rose, D. M., P. M. Cardarelli, R. R. Cobb, and M. H. Ginsberg. 2000. Soluble VCAM-1 binding to alpha4 integrins is cell-type specific and activation dependent and is disrupted during apoptosis in T cells. *Blood* 95: 602–609.
49. Nakao, S., T. Kuwano, T. Ishibashi, M. Kuwano, and M. Ono. 2003. Synergistic effect of TNF-alpha in soluble VCAM-1-induced angiogenesis through alpha 4 integrins. *J. Immunol.* 170: 5704–5711.
50. Wellicome, S. M., P. Kapahi, J. C. Mason, Y. Lebranchu, H. Yarwood, and D. O. Haskard. 1993. Detection of a circulating form of vascular cell adhesion molecule-1: raised levels in rheumatoid arthritis and systemic lupus erythematosus. *Clin. Exp. Immunol.* 92: 412–418.
51. McDonnell, G. V., S. A. McMillan, J. P. Douglas, A. G. Droogan, and S. A. Hawkins. 1998. Raised CSF levels of soluble adhesion molecules across the clinical spectrum of multiple sclerosis. *J. Neuroimmunol.* 85: 186–192.
52. Hamzaoui, A., J. Ammar, F. El Mekki, O. Borgi, H. Ghrairi, M. Ben Brahim, and K. Hamzaoui. 2001. Elevation of serum soluble E-selectin and VCAM-1 in severe asthma. *Mediators Inflamm.* 10: 339–342.

53. Kumasaka, T., W. M. Quinlan, N. A. Doyle, T. P. Condon, J. Sligh, F. Takei, Al. Beaudet, C. F. Bennett, and C. M. Doerschuk. 1996. Role of the intercellular adhesion molecule-1 (ICAM-1) in endotoxin-induced pneumonia evaluated using ICAM-1 antisense oligonucleotides, anti-ICAM-1 monoclonal antibodies, and ICAM-1 mutant mice. *J. Clin. Invest.* 97: 2362–2369.
54. Folkesson, H. G., and M. A. Matthay. 1997. Inhibition of CD18 or CD11b attenuates acute lung injury after acid instillation in rabbits. *J. Appl. Physiol* 82: 1743–1750.
55. Gao, X., N. Xu, M. Sekosan, D. Mehta, S. Y. Ma, A. Rahman, and A. B. Malik. 2001. Differential role of CD18 integrins in mediating lung neutrophil sequestration and increased microvascular permeability induced by *Escherichia coli* in mice. *J. Immunol.* 167: 2895–2901.
56. Tasaka, S., S. E. Richer, J. P. Mizgerd, and C. M. Doerschuk. 2002. Very late antigen-4 in CD18-independent neutrophil emigration during acute bacterial pneumonia in mice. *Am. J. Respir. Crit. Care Med.* 166: 53–60.
57. Singh, R. J., J. C. Mason, E. A. Lidington, D. R. Edwards, R. K. Nuttall, R. Khokha, V. Knauper, G. Murphy, and J. Gavrilovic. 2005. Cytokine stimulated vascular cell adhesion molecule-1 (VCAM-1) ectodomain release is regulated by TIMP-3. *Cardiovasc. Res.* 67: 39–49.
58. Rizzoni, D., M. L. Muiesan, E. Porteri, M. Castellano, M. Salvetti, C. Monteduro, C. De Ciuceis, G. Boari, U. Valentini, A. Cimino, et al. 2003. Circulating adhesion molecules and carotid artery structural changes in patients with noninsulin-dependent diabetes mellitus. *J. Hum. Hypertens.* 17: 463–470.
59. Atsuta, J., S. A. Sterbinsky, J. Plitt, L. M. Schwiebert, B. S. Bochner, and R. P. Schleimer. 1997. Phenotyping and cytokine regulation of the BEAS-2B human bronchial epithelial cell: demonstration of inducible expression of the adhesion molecules VCAM-1 and ICAM-1. *Am. J. Respir. Cell Mol. Biol.* 17: 571–582.
60. Vanderstocken, G., B. Bondue, M. Horckmans, L. Di Pietrantonio, B. Robaye, J. M. Boeynaems, and D. Communi. 2010. P2Y2 receptor regulates VCAM-1 membrane and soluble forms and eosinophil accumulation during lung inflammation. *J. Immunol.* 185: 3702–3707.
61. Lévesque, J. P., Y. Takamatsu, S. K. Nilsson, D. N. Haylock, and P. J. Simmons. 2001. Vascular cell adhesion molecule-1 (CD106) is cleaved by neutrophil proteases in the bone marrow following hematopoietic progenitor cell mobilization by granulocyte colony-stimulating factor. *Blood* 98: 1289–1297.